Progress in Reaction Kinetics and Mechanism

ARTICLE

Open Access

https://doi.org/10.48130/prkm-0026-0017

Progress in Reaction Kinetics and Mechanism **2026**, 51: e023

MFM-170 as an efficient adsorbent for the removal of thiophene S-based compounds from fuel oil

Han Chen[1,2], Yifang Sun[3], Yan Zhang[3], Yao Shen[4], Jingkai Zhao[4], Jiexu Ye[4*] and Shihan Zhang[4]

[1] *Nanxun Innovation Institute, Zhejiang University of Water Resources and Electric Power, Hangzhou 310018, China*
[2] *College of Environmental Science and Engineering, Zhejiang University of Water Resources and Electric Power, Hangzhou 310018, China*
[3] *College of Environment, Zhejiang University of Technology, Hangzhou 310014, China*
[4] *Zhejiang Key Laboratory of Clean Energy Conversion and Utilization, Science and Education Integration College of Energy and Carbon Neutralization, Zhejiang University of Technology, Hangzhou 310014, China*
* Correspondence: yejiexu@zjut.edu.cn (Ye J)

Abstract

Deep desulfurization of fuel oil is essential for environmental protection and clean energy production. Herein, to overcome the limitations of commonly used adsorbents for adsorption desulfurization, the metal–organic framework material MFM-170 was investigated for removing typical thiophene compounds, i.e., dibenzothiophene, 4-methyldibenzothiophene, and 4,6-dimethyldibenzothiophene, from simulated oil. A systematic optimization of the adsorption conditions revealed that at 40 °C and an oil-to-adsorbent ratio of 300, the adsorption of the three thiophene compounds on MFM-170 reached equilibrium within 5 min, with saturation adsorption capacity values of 57, 44, and 37 mg S/g. MFM-170 demonstrated excellent reusability, retaining 93% of its initial adsorption capacity for dibenzothiophene after seven adsorption–desorption cycles. The adsorption data were well fitted by the Freundlich isotherm model and the pseudo-second-order kinetic equation, indicating a multilayer adsorption process dominated by chemisorption. Mechanistic analyses revealed that the open Cu(II) active sites rapidly adsorb thiophene compounds via coordination to the S atoms and π–π stacking interactions. This study demonstrates the promising application potential of MFM-170 in the deep desulfurization of fuel oil.

Keywords: MFM-170, Adsorption desulfurization, Thiophene compounds, Adsorption kinetics, Metal–organic framework

Citation: Chen H, Sun Y, Zhang Y, Shen Y, Zhao J, et al. 2026. MFM-170 as an efficient adsorbent for the removal of thiophene S-based compounds from fuel oil. *Progress in Reaction Kinetics and Mechanism* 51: e023 https://doi.org/10.48130/prkm-0026-0017

Introduction

Sulfur oxides produced from the combustion of fuel oil contribute greatly to atmospheric pollution, directly harming human health and leading to decreased soil fertility and acid rain, thereby causing severe damage to ecosystems and infrastructure[1]. To address this environmental challenge, global regulations have substantially reduced permissible S concentrations in commercial fuels, with current limits reaching approximately 10 and 15 mg/kg in the EU and the US, respectively[2]. Given that SO_2 emissions primarily originate from the combustion of thiophene compounds in fuel oil, the development of technologies for the deep desulfurization of fuel oil has become an active area of research.

Among the desulfurization technologies, adsorption desulfurization has attracted widespread attention because of its low energy consumption, mild operating conditions, and high selectivity for specific S-containing compounds[3]. The effectiveness of this technology mainly depends on advanced adsorbent materials that can efficiently capture S-based compounds, with metal oxides[4], C-based materials[5], and zeolites[6] being the focus of current research. Although metal (M)-based adsorbents can chemically bind S-based compounds, their practical desulfurization efficiency and cycling stability are often limited by restricted active-site accessibility and slow diffusion kinetics[7]. Meanwhile, C-based materials predominantly rely on physisorption, leading to relatively low adsorption capacities and limited selectivity toward specific S species, especially under competitive adsorption conditions[8,9]. Zeolites are characterized by well-defined pore structures and tunable acidity; however, their effectiveness is constrained by pore size and diffusion limitations for bulky S-containing molecules as well as reduced stability in humid environments[10,11]. These limitations highlight the urgent need for developing efficient adsorbent materials.

Metal–organic frameworks (MOFs) are innovative porous materials composed of metal–oxide nodes, whose open metal sites can coordinate strongly with gas molecules. Furthermore, MOFs exhibit large specific surface areas and tunable pore architectures, rendering them promising adsorbents for adsorption desulfurization[7,12]. Among them, Cu-based MOFs exhibit outstanding adsorption performance. The π-complexation, acid–base interactions, and direct S–M interactions between Cu and S atoms enable the selective adsorption of organic S-based compounds[9]. For example, Blanco-Brieva et al. compared the desulfurization performance of Cu-BTC, Fe-BTC, and MIL-53(Al) and revealed that Cu-BTC exhibited the highest adsorption capacity[13]. Cychosz et al.[14] confirmed that the adsorption capacities of Cu-based MOFs, such as HKUST-1, UMCM-150, and MOF-505, for S-based compounds in isooctane exceeded those of Zn-based MOFs. Compared with these Cu-based MOFs, MFM-170 provides a more homogeneous and chemically tunable pore environment[1], which may be conducive to cooperative weak interactions during thiophene adsorption. This is favorable for reversible desulfurization under competitive conditions. However, the application of MFM-170 for the desulfurization of thiophene compounds has not yet been reported.

Herein, the MFM-170 adsorption performance toward representative thiophene compounds, specifically dibenzothiophene (DBT), 4-methyldibenzothiophene (4-MDBT), and 4,6-dimethyldibenzothiophene (DMDBT), was systematically evaluated. The impact of adsorption conditions on desulfurization efficiency was investigated, and

https://doi.org/10.48130/prkm-0026-0017

the adsorption mechanism was elucidated using adsorption kinetics and isotherm studies. Furthermore, the reusability of MFM-170 was assessed by conducting cyclic desorption–adsorption experiments. The structure–activity relationship was comprehensively investigated using competitive adsorption experiments and structural characterization. This study provides theoretical and experimental insights into the potential implementation of MFM-170 in the deep desulfurization of fuel oil.

Materials and methods

Materials

All precursors were used as received without additional purification. DBT (≥ 99%), DMDBT (97%), n-octane (> 99% [GC]), ethanol (≥ 99.8%), *N*,*N*-dimethylformamide (DMF, ≥ 99.9%), methanol (≥ 99.9%), nitric acid (HNO_3, 65%–68%), and copper(II) nitrate hemipentahydrate ($Cu[NO_3]_2{\cdot}2.5\ H_2O$, 99.7%) were acquired from Shanghai Aladdin Biochemical Technology Co., Ltd. 4-MDBT (97%) was obtained from Beijing Bailingwei Technology Co., Ltd. Acetone (≥ 99.9%) was obtained from Shanghai Titan Scientific Co., Ltd. 4',4'''-(Pyridine-3,5-diyl)bis([1,1'-biphenyl]-3,5-dicarboxylic acid) (H_4L, 97%) was sourced from Shanghai Bide Pharmatech Co., Ltd. High-purity N_2 (99.999%) and synthetic air (99.999%) were obtained from Hangzhou Jinte Special Gas Co., Ltd.

Preparation of MFM-170

Following the method reported by Smith et al.[1], $Cu(NO_3)_2{\cdot}2.5\ H_2O$ (298 mg, 1.28 mmol) and H_4L (192 mg, 0.36 mmol) were added to 48 mL of a solvent mixture of water and DMF with a volume ratio of 1:5, and 0.3 mL of HNO_3 was added for acidification. The resulting mixture was transferred to a glass vial and reacted at 80 °C for 18 h, yielding blue octahedral crystals of MFM-170. Subsequently, the as-synthesized MFM-170 was activated to remove solvent molecules and residual reactants as follows[15]. First, the material was washed with a hot DMF solution under constant stirring at 60 °C and then immersed in acetone at room temperature for 1 week, with the acetone being replaced every 12 h. After immersion, the sample was transferred to a vacuum drying oven and heated at 80 °C for 6 h to obtain a preliminarily activated material. Before adsorption performance testing, an appropriate amount of sample was weighed and activated in a vacuum drying oven at 150 °C for 12 h to eliminate solvent molecules and most coordinated water from the pores, ultimately yielding fully activated MFM-170.

Characterization of the adsorbent

The crystalline structure of MFM-170 was characterized using X-ray diffraction (XRD; Rigaku SmartLab 9 kW, Japan) with a Cu target as the radiation source, scanning from $2\theta = 5°$ to 30° at a scan rate of 2°/min. Fourier transform infrared (FT-IR) spectroscopy (Thermo Scientific Nicolet iS20, USA) was employed to identify the functional groups of MFM-170 in the wavenumber range of 4,000–700 cm^{-1}. Thermogravimetric analysis (TGA; TGA/DSC 3+, Mettler Toledo, Switzerland) was performed to investigate the thermal stability and component content of MFM-170 under air. Before testing, the sample was preheated at 80 °C under N_2. For measurement, the temperature was increased from 25 to 800 °C at a ramp rate of 5 °C/min with an airflow rate of 20 mL/min. Scanning electron microscopy (SEM; ZEISS Sigma 300, Germany) was employed to examine the surface topology and microstructural characteristics of MFM-170. X-ray photoelectron spectroscopy (XPS; Thermo Scientific K-Alpha, USA) was used to determine the surface composition and valence states. The N_2 adsorption–desorption isotherms were measured at 77.3 K using a fully automatic four-station specific surface area analyzer (Micromeritics ASAP 2460, USA).

Adsorption desulfurization experiments

Simulated oils with varying S contents were prepared by separately dissolving DBT, 4-MDBT, and DMDBT at various concentrations in n-octane at room temperature. The concentration of the simulated oil was calculated using Eq. (1) as follows:

$$c = \frac{M_S \times m \times 1{,}000}{M \times V} \tag{1}$$

where, c is the simulated oil concentration (mg S/g), m denotes the mass of the corresponding thiophene compound (g), M_S indicates the molar mass of S (g), M is the molar mass of the corresponding thiophene compound (g), and V is the volume of the simulated oil (L).

Adsorption desulfurization experiments were conducted in a constant-temperature water bath. Activated MFM-170 was placed in a 9-mL sample vial, and a certain volume of simulated oil was added, followed by oscillatory adsorption at a set temperature. Samples were taken at predetermined time points, filtered through a membrane, and collected in sample vials, and the S content was determined using gas chromatography (GC; Agilent 8890 GC, USA). The analytical parameters were set as follows: an HP-5 capillary column for separation, a flame ionization detector (FID) for detection, N_2 as the carrier gas with a flow rate of 0.65 mL/min, and an injection volume of 0.7 μL. For the DBT analysis, the injector and FID temperatures were set at 290 °C, and the oven temperature ranged from 160 to 260 °C. For 4-MDBT and DMDBT analyses, the injector and FID temperatures were set at 300 °C, and the oven temperature ranged from 160 to 290 °C. For quantitative analysis, standard solutions of the thiophene compounds with different concentrations were prepared. After GC analysis, a calibration curve of peak area vs. S concentration was constructed ($R^2 \geq 0.999$). Using this curve, the concentration difference was calculated according to the change in the peak area of S in the simulated oil before and after adsorption. Then, the specific adsorption capacity of MFM-170 was calculated using Eq. (2) as follows:

$$q_e = \frac{(c_0 - c_e) \times V}{m} \tag{2}$$

where, q_e represents the equilibrium adsorption capacity of the adsorbent (mg S/g), c_0 indicates the initial S concentration of the simulated oil (mg S/L), c_e denotes the S concentration of the simulated oil at adsorption equilibrium (mg S/L), V is the volume of the simulated oil (L), and m is the mass of the adsorbent (g).

In competitive adsorption experiments, to quantitatively evaluate the adsorption selectivity of MFM-170 for DBT, the distribution coefficient (K_d, L/g) was calculated using Eq. (3)[16].

$$K_d = \frac{q_e}{c_e} \tag{3}$$

The adsorption isotherms were fitted and analyzed using the Langmuir (Eqs. [4] and [5]) and Freundlich (Eqs. [6] and [7]) isothermal adsorption models.

$$q_e = \frac{q_m c_e K_L}{1 + K_L c_e} \tag{4}$$

$$\frac{c_e}{q_e} = \frac{c_e}{q_m} + \frac{1}{q_m K_L} \tag{5}$$

$$q_e = K_F c_e^{1/n} \tag{6}$$

$$\ln q_e = \ln K_F + \frac{1}{n} \ln c_e \quad (7)$$

In these equations, q_m is the Langmuir monolayer saturation adsorption capacity (mg S/g), K_L represents the Langmuir constant, and K_F is the Freundlich constant.

The adsorption kinetic process was fitted using the pseudo-first-order kinetic model (Eq. [8]), pseudo-second-order kinetic model (Eq. [9]), and intraparticle diffusion model (Eq. [10]) as follows:

$$\ln (q_e - q_t) = \ln q_e - k_1 t \quad (8)$$

$$q_t = \frac{q_e^2 k_2 t}{1 + q_e k_2 t} \quad (9)$$

$$q_t = k_{id} t^{0.5} + C \quad (10)$$

where, q_t indicates the adsorption capacity of the adsorbent at time t (mg S/g), k_1 represents the pseudo-first-order adsorption rate constant, k_2 is the pseudo-second-order adsorption rate constant, k_{id} represents the intraparticle diffusion rate constant, t indicates the time (s), and C is the intercept (mg/g).

All adsorption desulfurization experiments were performed in triplicate, and the data are presented as the mean ± standard deviation.

Results and discussion

Analysis of MFM-170

The SEM images (Fig. 1a) of the synthesized MFM-170 sample reveal a regular crystalline morphology with high crystallinity, distinct crystal faces, and relatively large, uniformly distributed crystals. These results demonstrate that the synthesis and activation procedures used in this study successfully produced MFM-170 with a well-defined crystal structure, providing a reliable morphological foundation for subsequent investigation of the adsorption performance.

Figure 1b confirms that the characteristic peaks shown in the XRD pattern of the synthesized MFM-170 sample show excellent agreement with those of the standard reference, further verifying its phase purity and structural correctness.

The thermal stability of MFM-170 was evaluated via TGA (Fig. 1c). A mass loss of approximately 4.7% was observed between room temperature and 150 °C, primarily owing to the removal of physically adsorbed solvent molecules and some coordinated water from the material pores. Further weight loss of approximately 10.4% occurred between 150 and 350 °C, corresponding to the gradual removal of residual solvent molecules and strongly coordinated water from the channels, indicating the presence of binding sites that require higher temperatures for complete activation. When the temperature exceeded 350 °C, the framework structure began to collapse, as evidenced by a substantial mass loss of approximately 60.3% between 350 and 500 °C, indicating irreversible decomposition of the MFM-170 framework. Overall, MFM-170 exhibits good thermal stability, maintaining its framework structure up to 350 °C, which supports its potential applications in high-temperature adsorption and catalytic processes. Furthermore, the TGA results indicate the presence of strong coordination interactions between the Cu(II) sites and solvent molecules; therefore, high-temperature and vacuum conditions are required for complete activation and exposure of additional active sites. This is consistent with previous

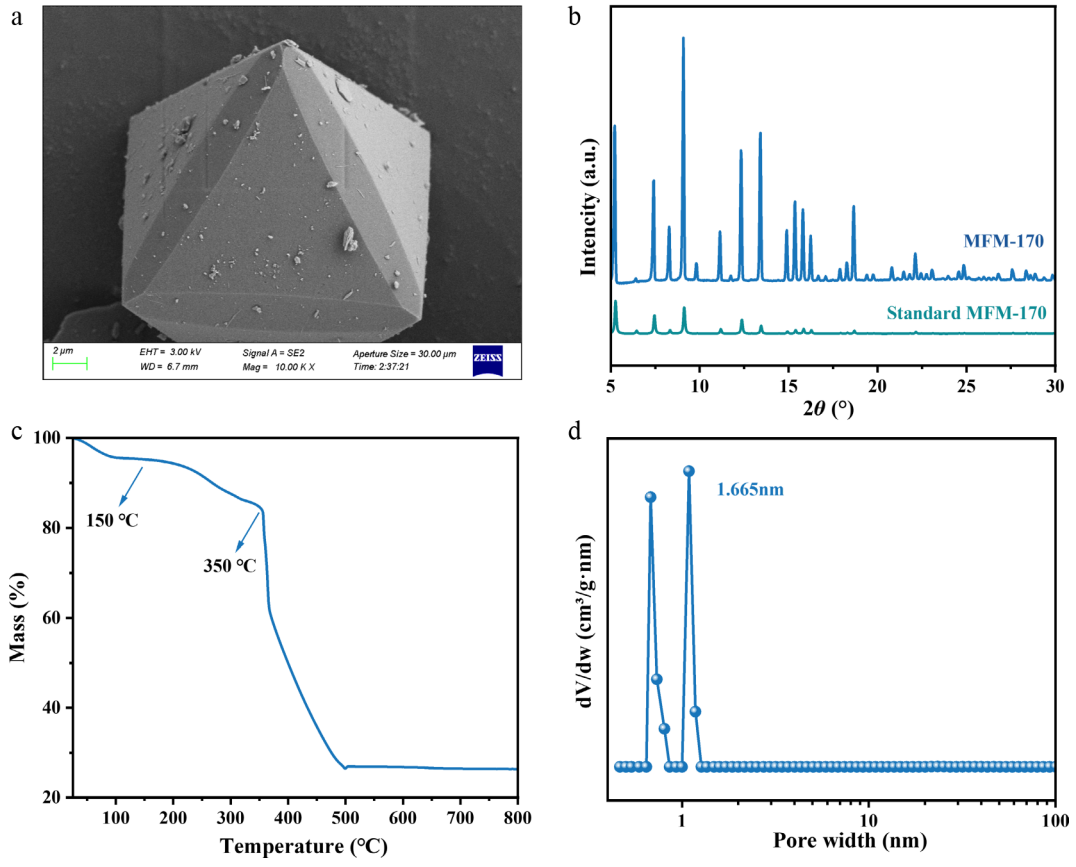

Fig. 1 Characterization results obtained for MFM-170, including (a) SEM images, (b) XRD profile, (c) TGA curve, and (d) pore size distribution diagram.

https://doi.org/10.48130/prkm-0026-0017

studies indicating that the proportion of open metal sites increases with increasing activation temperature, enhancing adsorption and catalytic performance[17].

BET analysis was performed to clarify the textural properties of activated MFM-170 (Fig. 1d). The calculated BET surface area was 1,165.7 m^2/g. The total pore volume reached 0.485 cm^3/g at P/P_0 = 0.995, while t-plot analysis gave a micropore area of 1,116.3 m^2/g and a micropore volume of 0.424 cm^3/g, confirming that the accessible porosity mainly originates from micropores. The average pore diameter calculated by the 4V/A method was 1.665 nm, and the pore size distribution was mainly located below 2 nm, consistent with the IUPAC definition of micropores. These results demonstrate that activated MFM-170 possesses substantial accessible surface area and confined microporous volume, which are favorable for the enrichment of sulfur-containing compounds and their interaction with Cu sites.

Adsorption performance

To systematically investigate the optimal adsorption conditions for MFM-170, the effects of oil-to-adsorbent ratio, temperature, and adsorption time on adsorption capacity were examined. The experiments were conducted using DBT as the thiophene compound and n-octane as the solvent, with a S concentration in the simulated oil of 1,000 mg S/L.

Figure 2a shows the impact of the oil-to-adsorbent ratio (50–350) on the adsorption of DBT on MFM-170 at 40 °C. As the oil-to-adsorbent ratio increased, the adsorption capacity gradually increased and then stabilized when the ratio exceeded 250, indicating saturation of the active sites. Therefore, the optimal oil-to-adsorbent ratio was determined to be 300. Under this condition, the impact of temperature on the adsorption behavior was studied (Fig. 2b). The adsorption capacity initially increased and then decreased with increasing temperature, reaching its maximum at 40 °C. This trend reflects the synergistic effect of physisorption and chemisorption: increasing temperature facilitates the diffusion of DBT molecules to open Cu(II) sites, promoting chemisorption; however, excessively high temperatures weaken physisorption, leading to an overall decline in adsorption performance[18]. Thus, the optimal adsorption temperature was set at 40 °C. Figure 2c shows the variation in adsorption capacity with time at an oil-to-adsorbent ratio of 300 and an adsorption temperature of 40 °C. The adsorption of DBT on MFM-170 was rapid, reaching 40 mg S/g within 5 s, increasing to 50 mg S/g within 1 min, and then slowing down until reaching adsorption equilibrium (approximately 57 mg S/g) after about 5 min. Therefore, the optimal adsorption time was determined to be 5 min.

Under the optimal adsorption conditions of an oil-to-adsorbent ratio of 300 and a temperature of 40 °C, the adsorption performance of MFM-170 for the three thiophene compounds was further investigated. As shown in Fig. 3a, MFM-170 exhibited rapid adsorption kinetics for DBT (1,000 mg S/L), 4-MDBT (600 mg S/L), and DMDBT (600 mg S/L), reaching adsorption equilibrium within approximately 240 s, with saturation adsorption capacities of 57, 44, and 37 mg S/g, respectively. The adsorption capacity decreased with increasing molecular size and steric hindrance. The steric effects of the methyl group in 4-MDBT and DMDBT limited their effective contact with the adsorption active sites[19]. Consequently, the adsorption capacities of MFM-170 for 4-MDBT and DMDBT were considerably lower than that for DBT. The adsorption performance of MFM-170 for DBT was systematically compared with that of previously reported adsorbents. As shown in Fig. 3b and Table 1, the adsorption capacity of MFM-170 (57 mg S/g) exceeded that of activated carbons, zeolites, and other MOF materials, demonstrating the immense potential of MFM-170 for practical application in deep desulfurization of fuel oils.

To evaluate the adsorption selectivity of MFM-170 in complex systems, considering that the aromatic content in fuel compositions typically ranges from 20 to 30 wt%, the effect of toluene as a representative competitive component on DBT adsorption was investigated. Toluene at 10, 15, 20, and 25 wt% was separately added to the model oil with a DBT S concentration of 1,000 mg S/L, and the adsorption experiment was conducted under the optimized conditions for 12 h. As shown in Fig. 3c, toluene substantially decreased the DBT adsorption capacity of MFM-170. In particular, when the toluene content was 25 wt%, the adsorption capacity for DBT was 31 mg S/g, representing a decrease of approximately 46% compared to that of the toluene-free system, and the K_d value dropped from 0.20 to 0.03 L/g. These results indicate that toluene and DBT compete for the adsorption sites on MFM-170. The competition mechanism primarily stems from the ability of toluene, as an aromatic hydrocarbon compound, toluene can engage in π–π stacking interactions with the aromatic rings within the MFM-170 framework and interact with the open Cu(II) sites[29,30]. This result confirms that coexisting aromatic hydrocarbon components in practical fuel oil systems can substantially affect the desulfurization performance of MFM-170.

To further explore the role of open Cu(II) sites in MFM-170, the adsorption performance of three typical thiophene compounds was compared before and after dehydration treatment. MFM-170 was activated under vacuum at 150 °C for 12 h to effectively remove coordinated water and residual solvent molecules from the pores,

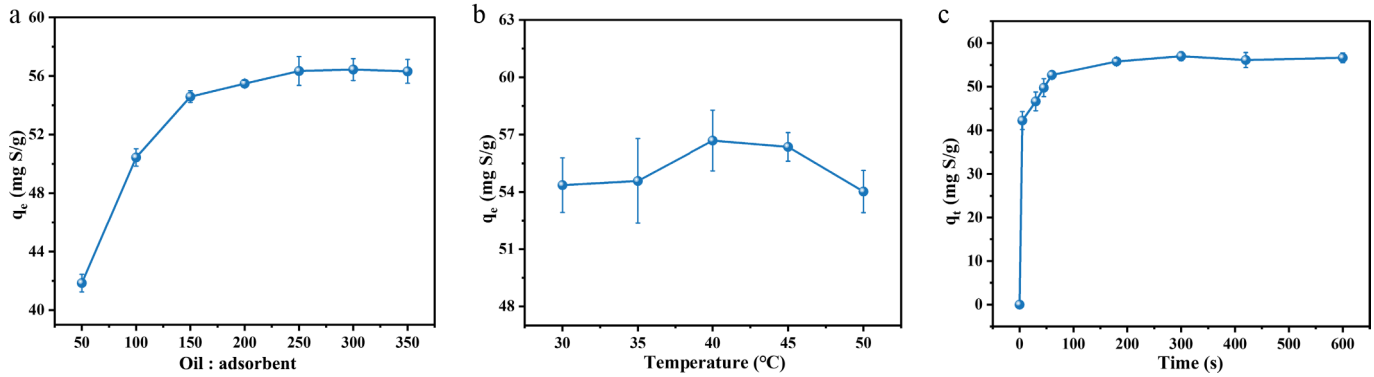

Fig. 2 (a) Adsorption capacity of MFM-170 for DBT vs. oil-to-adsorbent ratio; (b) adsorption capacity of MFM-170 for DBT vs. temperature; (c) adsorption capacity of MFM-170 for DBT vs. time.

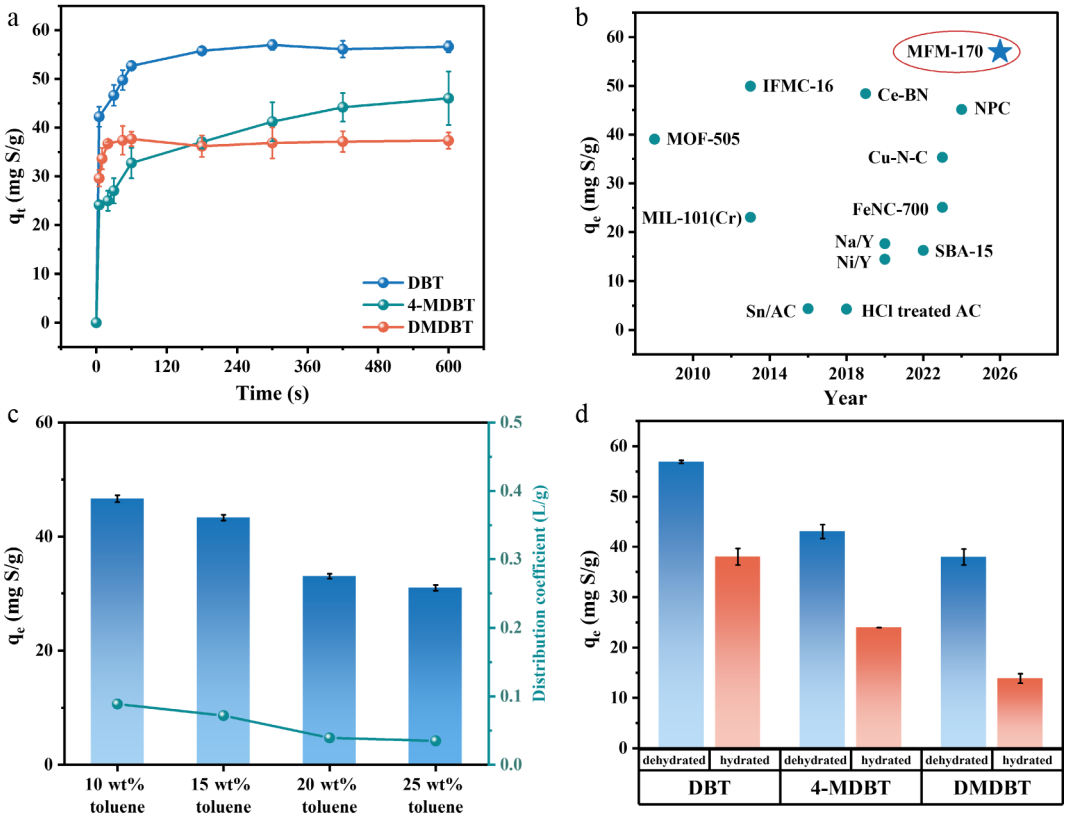

Fig. 3 (a) Adsorption capacity of MFM-170 for DBT, 4-MDBT, and DMDBT vs. time; (b) DBT adsorption capacity comparison of MFM-170 and reported adsorbents (detailed comparisons are presented in Table 1); (c) effect of toluene competitive adsorption on the adsorption capacity and distribution coefficient of DBT; (d) effect of adsorbed water on adsorption performance.

Table 1. Comparison of the DBT adsorption capacity on various materials.

Sample	Adsorbate	Adsorption capacity (mg S/g)	Ref.
MOF-505	DBT	39.04	[14]
MIL-101(Cr)	DBT	23.04	[20]
SBA-15	DBT	16.23	[21]
Ce-BN	DBT	48.40	[22]
NPC	DBT	45.14	[23]
FeNC-700	DBT	25.08	[24]
IFMC-16	DBT	49.92	[25]
Cu-N-C	DBT	35.32	[26]
HCl treated AC	DBT	4.28	[27]
Sn/AC	DBT	4.35	[28]
Na/Y	DBT	17.63	[11]
Ni/Y	DBT	14.43	[11]
MFM-170	DBT	57.00	This work

fully exposing the Cu(II) open sites. Subsequently, tests were conducted under identical adsorption conditions (40 °C and an oil-to-adsorbent ratio of 300 for 12 h). As illustrated in Fig. 3d, dehydration substantially enhanced the adsorption capacity of MFM-170 for all thiophene compounds. In particular, the adsorption capacities for DBT, 4-MDBT, and DMDBT increased by 33%, 44%, and 63% from 38.0, 23.9, and 13.8 mg S/g to 56.9, 43.0, and 37.9 mg S/g, respectively. Notably, the adsorption capacity for DMDBT showed the most pronounced enhancement after dehydration, indicating that the open Cu(II) sites exhibited better adsorption efficiency for thiophene compounds with greater steric hindrance. Nondehydrated MFM-170 primarily relies on physical adsorption and π–π stacking interactions to capture thiophene compounds, whereas dehydrated MFM-170 shows markedly enhanced adsorption efficiency owing to coordination interactions between the exposed Cu(II) sites and S atoms[1,31]. These results thoroughly demonstrate the crucial role of open Cu(II) sites in achieving highly selective adsorption.

To further evaluate the practical application potential of MFM-170, systematic investigations were conducted on its cycling stability and structural durability. Cycling experiments were performed using DBT (1,000 mg S/L) in n-octane simulated oil under optimal adsorption conditions for 12 h. After each adsorption cycle, the sample was restored via Soxhlet extraction with methanol for 12 h and then vacuum-dried at 150 °C for another 12 h. As shown in Fig. 4, after seven cycles, the adsorption capacity of MFM-170 for DBT was 53 mg S/g, corresponding to 93% of the initial adsorption capacity (57 mg S/g), indicating excellent regeneration performance.

The structural changes of MFM-170 after adsorption were analyzed via FT-IR spectroscopy (Fig. 5a). The wide band at 3,500 cm^{-1} can be ascribed to the O–H stretching vibration. The strong bands at 1,300–1,700 cm^{-1} are associated with the –(O–C–O)– groups of dicarboxylate linkers and the C=C vibrations of benzene rings. The bands at 1,020 and 1,070 cm^{-1} are characteristic of C–O–Cu vibrations, and the bands at 730 and 760 cm^{-1} are owing to Cu–O vibrations, consistent with previous reports[32]. The appearance of new bands at 870 and 920 cm^{-1} after adsorption indicates the formation of S–Cu coordination between MFM-170 and DBT, confirming the crucial role of Cu(II) sites in the adsorption process. Simultaneously, the enhanced peak intensities after adsorption are attributable to interactions between the acidic groups of MFM-170 and the thiophene compounds. High-resolution Cu 2p XPS spectra were further collected to probe the chemical interaction between sulfur species

https://doi.org/10.48130/prkm-0026-0017

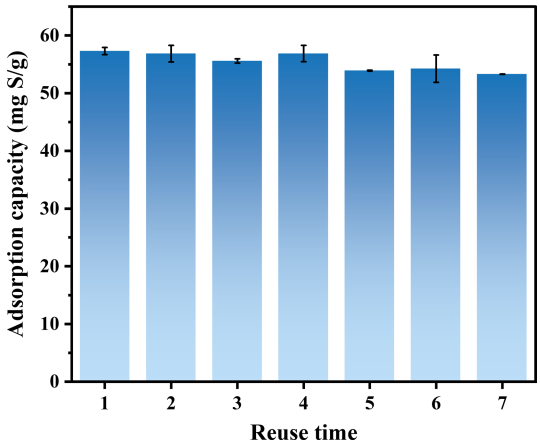

Fig. 4 Recycling performance of MFM-170.

and Cu sites (Fig. 5b). For fresh MFM-170, the Cu $2p_{3/2}$ envelope can be deconvoluted into Cu(I)-like and Cu(II) components, accompanied by typical shake-up satellites in the 940–945 eV region, confirming the coexistence of reduced Cu species and Cu(II) centers. After use, the Cu 2p profile changed markedly. A new component appeared in the Cu $2p_{3/2}$ region at ca. 933 eV, together with its corresponding Cu $2p_{1/2}$ contribution, which can be assigned to S–Cu species. Meanwhile, the Cu(I)/Cu(II) components shifted slightly toward lower binding energy, indicating increased electron density around Cu centers and partial reduction of Cu(II) during interaction with sulfide species. Such negative shifts and the emergence of S–Cu-related Cu 2p signals are consistent with reported Cu-based MOFs after H_2S adsorption, where S^{2-} coordination induces S–Cu bond formation and lowers the Cu 2p binding energy[33]. The S 2p spectrum of used MFM-170 (Fig. 5c) was fitted using spin–orbit doublets with a fixed splitting of 1.18 eV and an area ratio of 2:1 for S $2p_{3/2}$/S $2p_{1/2}$. A low-binding-energy doublet with S $2p_{3/2}$ located at ca. 161.7–162.4 eV can be assigned to sulfide-like sulfur coordinated to Cu sites, i.e., S–Cu species[34]. Together with the negative shift and newly resolved S–Cu-related contribution in the Cu 2p spectrum, the S 2p results provide evidence that sulfur species generated during adsorption interact with Cu centers in MFM-170, further confirming the formation of S–Cu coordination. An XRD analysis of the sample after seven cycles (Fig. 5d) confirmed that the intensity of the characteristic diffraction peaks substantially decreased, accompanied by peak broadening, indicating partial collapse of the crystalline structure and reduced crystallinity during multiple adsorption–regeneration cycles. However, MFM-170 still maintained relatively good adsorption performance, demonstrating promising application potential.

Adsorption behavior and mechanism

In adsorption studies, adsorption isotherms describe the release or movement of compounds from aqueous porous media into the solid phase of the adsorbent at a constant temperature. As the phase containing the adsorbate interacts with the adsorbent for a sufficient period of time, adsorption equilibrium—the ratio between

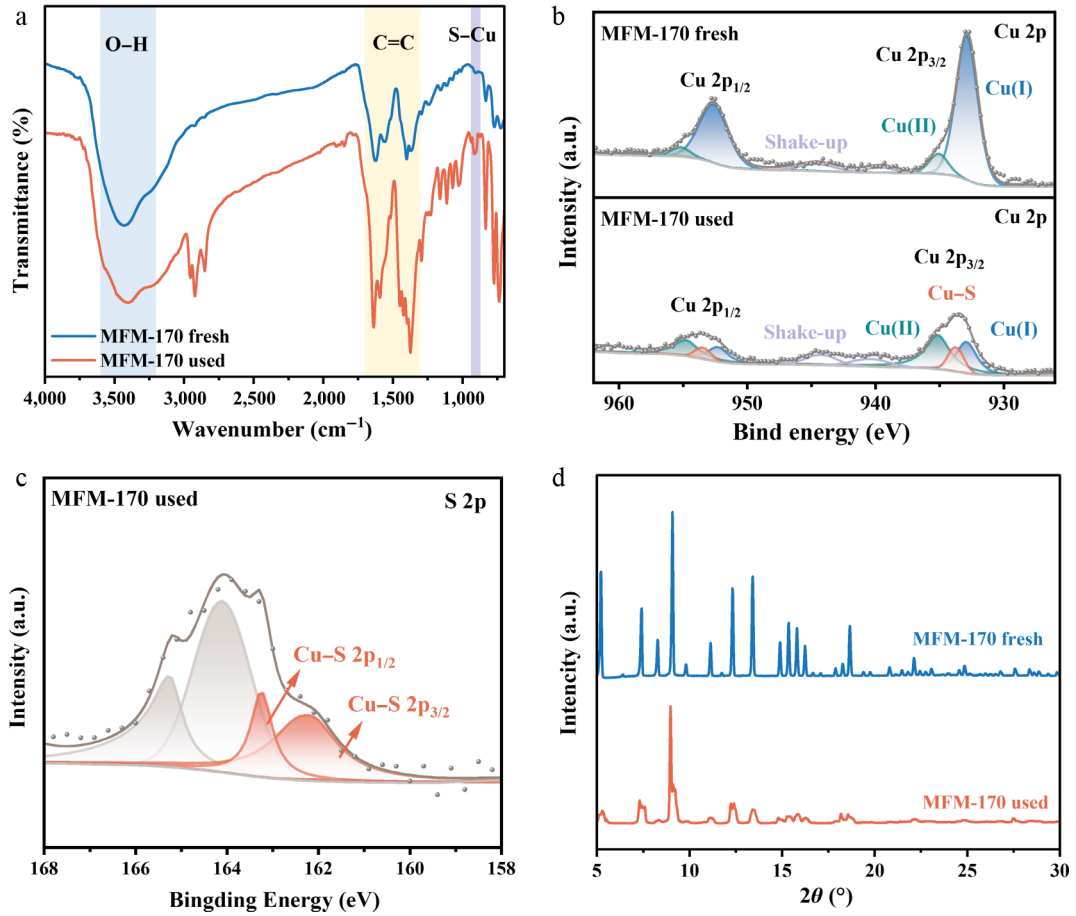

Fig. 5 (a) FT-IR profiles of fresh and used MFM-170; (b) Cu 2p XPS spectra of fresh and used MFM-170; (c) S 2p XPS spectrum of used MFM-170; (d) XRD profiles of fresh and used MFM-170.

the amount adsorbed and that remaining in the solution—is reached. At this stage, the adsorbate content in the bulk solution is in dynamic equilibrium with the interfacial concentration[35]. To investigate the adsorption behavior and mechanism of MFM-170 for the thiophene compounds, adsorption isotherms were measured for DBT, 4-MDBT, and DMDBT at 30, 40, and 50 °C (Fig. 6a, d, g). The adsorption capacity considerably improved with increasing equilibrium concentration of the thiophene compounds and gradually approached saturation. Excellent adsorption performance was observed even at higher concentrations, indicating the remarkable adsorption potential of MFM-170.

The Langmuir (Fig. 6b, e, h) and Freundlich (Fig. 6c, f, i) models were used to analyze the isothermal adsorption data. Table 2 shows that the R^2 value for the Freundlich model was generally above 0.99, substantially higher than that for the Langmuir model. This demonstrates that the adsorption behavior of MFM-170 for the three thiophene compounds conforms more closely to the Freundlich isothermal adsorption model, which describes reversible, nonideal chemisorption on heterogeneous adsorbent surfaces. This model is not limited to a monolayer; instead, it describes multilayer adsorption on heterogeneous surfaces in which the heat of adsorption and adsorption affinity are unevenly distributed, with the adsorption capacity decreasing as the active sites become occupied. According to the Freundlich adsorption model, at different concentrations, the ratio of the amount adsorbed by a given mass of adsorbent to the solute is not constant. As adsorption proceeds, the adsorbent preferentially occupies high-energy sites, and the adsorption intensity decreases exponentially with increasing site occupancy, eventually reaching adsorption equilibrium. The 1/n values obtained using the Freundlich model ranged between 0 and 1, indicating that multilayer adsorption was preferable and the adsorbent surface possessed active sites with an uneven energy distribution[36,37]. Furthermore, among the three thiophene compounds, DBT showed the highest K_F value, demonstrating the strongest adsorption capacity of MFM-170 for DBT. In contrast, 4-MDBT and DMDBT exhibited relatively lower K_F values owing to their steric hindrance.

The adsorption kinetics of MFM-170 were systematically investigated to evaluate its practical potential for industrial applications. As shown in Fig. 7a, b, the pseudo-first-order and pseudo-second-order kinetic models were used to fit the experimental data. The pseudo-second-order kinetic model demonstrated an appropriate fit for the adsorption of DBT, 4-MDBT, and DMDBT, with R^2 values greater than 0.99. This result confirms that adsorption on MFM-170 is primarily governed by chemisorption[38], including electron

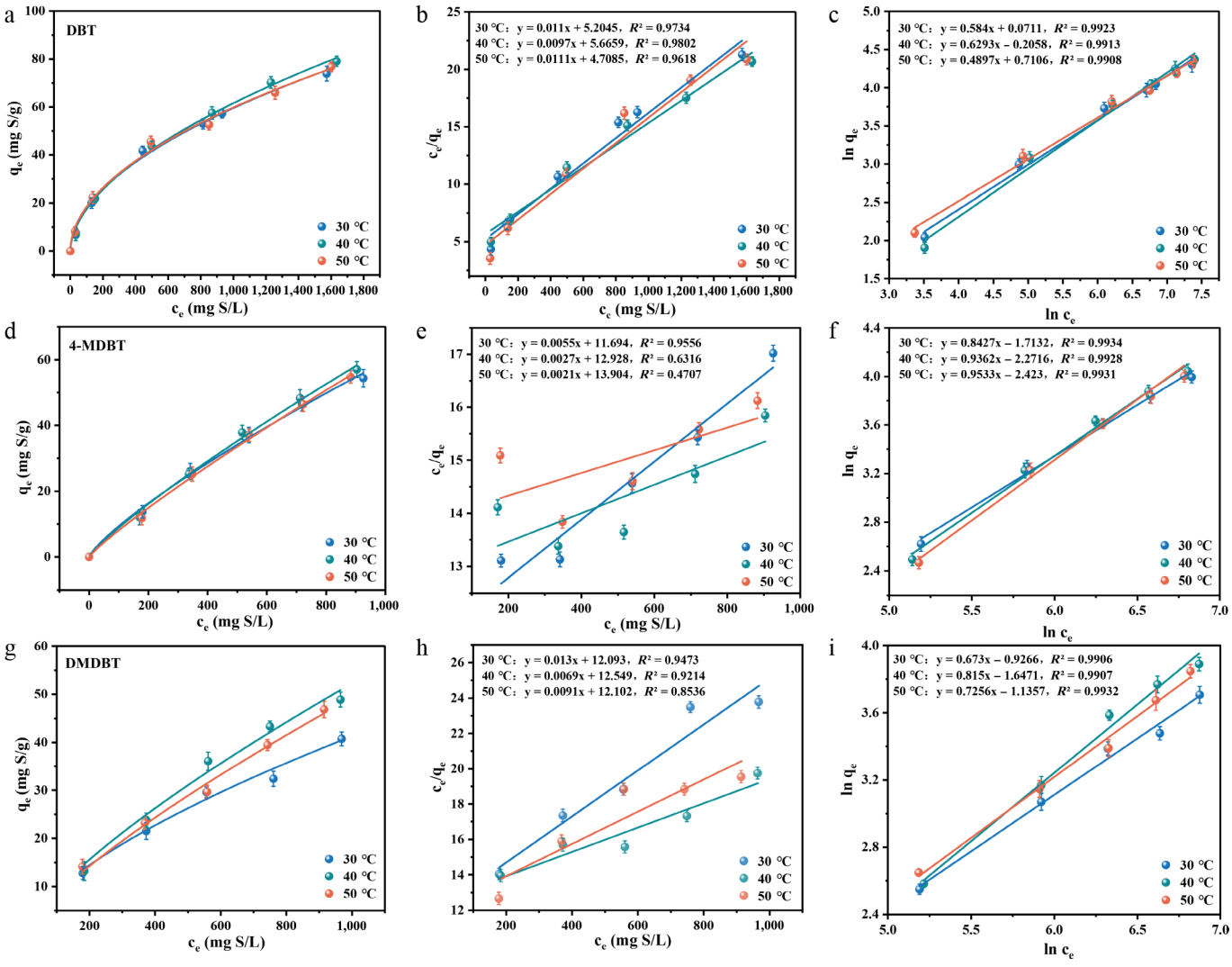

Fig. 6 Adsorption isotherms of (a) DBT, (d) 4-MDBT, and (g) DMDBT on MFM-170; Langmuir model fitting plots for (b) DBT, (e) 4-MDBT, and (h) DMDBT on MFM-170; Freundlich model fitting plots for (c) DBT, (f) 4-MDBT, and (i) DMDBT on MFM-170.

https://doi.org/10.48130/prkm-0026-0017

Table 2. Fitted parameters of Langmuir and Freundlich models.

Temperature (°C)	Adsorbates	Langmuir			Freundlich		
		q_{max} (mg S/g)	K_L	R^2	K_F	n	R^2
30	DBT	90.91	0.0021	0.9734	1.0737	1.7123	0.9923
	4-MDBT	181.82	0.0005	0.9556	0.1803	1.1867	0.9934
	DMDBT	76.92	0.0011	0.9473	0.3960	1.4859	0.9906
40	DBT	103.09	0.0017	0.9802	0.8140	1.5891	0.9913
	4-MDBT	370.37	0.0002	0.6316	0.1031	1.0681	0.9928
	DMDBT	144.93	0.0005	0.9214	0.1926	1.2270	0.9907
50	DBT	90.09	0.0023	0.9618	2.0352	2.0421	0.9908
	4-MDBT	476.19	0.0002	0.4707	0.0887	1.0490	0.9931
	DMDBT	109.89	0.0007	0.8536	0.3212	1.3782	0.9932

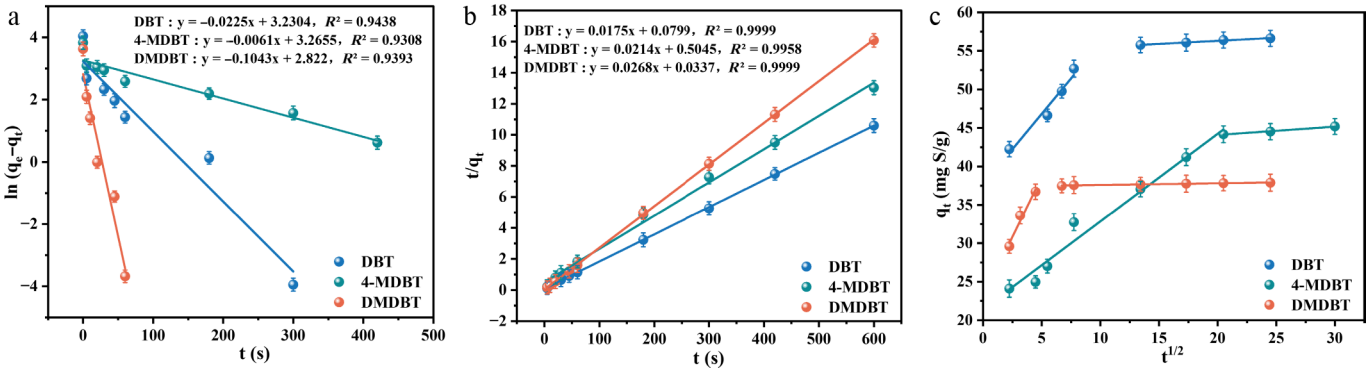

Fig. 7 Kinetic models for the adsorption of DBT, 4-MDBT, and DMDBT on MFM-170: (a) pseudo-first-order model, (b) pseudo-second-order model, and (c) Weber–Morris intraparticle diffusion model.

Table 3. Kinetic parameters of the Weber–Morris intraparticle diffusion model for the adsorption of DBT, 4-MDBT, and DMDBT on MFM-170.

Adsorbates	Adsorption stage	Fitting equation	K_{id} (mg S/g/min$^{0.5}$)	C (mg S/g)	R^2
DBT	1	$y = 1.8363x + 37.651$	1.8363	37.651	0.9646
	2	$y = 0.0801x + 54.698$	0.0801	54.698	0.9868
4-MDBT	1	$y = 1.1392x + 21.457$	1.1392	21.457	0.9755
	2	$y = 0.1075x + 41.939$	0.1075	41.939	0.9920
DMDBT	1	$y = 3.1243x + 23.029$	3.1243	23.029	0.9701
	2	$y = 0.0222x + 37.367$	0.0222	37.367	0.9691

sharing or transfer between adsorbate and adsorbent. In addition, the R^2 value for the pseudo-first-order kinetic model was approximately 0.9, demonstrating that adsorbate diffusion in the liquid film influences the overall adsorption rate[37].

The kinetic data were fitted to the Weber–Morris intraparticle diffusion model to further study the mass transfer mechanism (Fig. 7c; Table 3). None of the fitted lines passed through the origin ($C > 0$), indicating that intraparticle diffusion is not the only rate-controlling step of the adsorption process. The relatively large C values reflect a marked boundary-layer effect, demonstrating that the external surface of MFM-170 can rapidly bind S-containing molecules. This is facilitated by the abundant phenyl ring structures within its framework, providing π–π interaction sites, and by the chemical affinity generated by the coordinatively unsaturated Cu sites[37].

This analysis revealed that the adsorption of thiophene compounds on MFM-170 proceeds via two consecutive steps: a prompt surface adsorption stage, where thiophene molecules instantaneously attach to the external surface of MFM-170, and an internal diffusion and binding stage, where molecules migrate through the pores to the material interior and bind with active sites until adsorption equilibrium is reached. This mechanism explains the high adsorption capacity and rapid kinetics of MFM-170.

Conclusions

The MFM-170 adsorption performance for thiophene compounds in fuel oil was systematically investigated. MFM-170 exhibited high adsorption capacity and rapid adsorption kinetics for DBT, 4-MDBT, and DMDBT. Moreover, it retained 93% of its initial adsorption capacity after seven adsorption–desorption cycles, revealing excellent reusability. Kinetic studies demonstrated that the adsorption of DBT, 4-MDBT, and DMDBT on MFM-170 adhered to the Freundlich isotherm model and the pseudo-second-order kinetic model, indicating that the process was mainly governed by chemisorption. Mechanistic studies demonstrated that the outstanding performance of MFM-170 originates from its phenyl ring structures and open Cu(II) active sites. Although MFM-170 demonstrated highly competitive desulfurization performance, its transition from the laboratory to industrial application still faces practical challenges. From a sustainability perspective, the organic ligands used in the MFM-170 synthesis represent a non-negligible cost factor. Therefore, a life cycle assessment should be conducted for the entire synthesis–adsorption–regeneration process to systematically evaluate the economic and environmental feasibility of its large-scale deployment. Future research should focus on optimizing the MOF synthesis strategy for low-cost, large-scale production.

Author contributions

The authors confirm their contributions to the paper as follows: writing – original draft, funding acquisition: Chen H; formal analysis: Sun Y; experiment conduction: Sun Y, Zhang Y; data curation: Shen Y; supervision: Zhao J, Ye J, Zhang S; conceptualization, writing – review and editing: Ye J. All authors reviewed the results and approved the final version of the manuscript.

Data availability

All data generated or analyzed during this study are included in this published article.

Acknowledgments

We appreciate the funding support from the National Natural Science Foundation of China (21906151), the Nanxun Scholars Program of ZJWEU (RC2024010930), and the Ningbo Natural Science Foundation (2024J445).

Conflict of interest

The authors declare that they have no conflict of interest.

Dates

Received 5 February 2026; Revised 10 May 2026; Accepted 15 June 2026; Published online 4 August 2026

References

[1] Smith GL, Eyley JE, Han X, Zhang X, Li J, et al. 2019. Reversible coordinative binding and separation of sulfur dioxide in a robust metal-organic framework with open copper sites. *Nature Materials* 18:1358–1365

[2] Ahmed I, Jhung SH. 2016. Adsorptive desulfurization and denitrogenation using metal-organic frameworks. *Journal of Hazardous Materials* 301:259–276

[3] Danmaliki GI, Saleh TA, Shamsuddeen AA. 2017. Response surface methodology optimization of adsorptive desulfurization on nickel/activated carbon. *Chemical Engineering Journal* 313:993–1003

[4] Liao J, Wang Y, Chang L, Bao W. 2015. Preparation of M/γ-Al_2O_3 sorbents and their desulfurization performance in hydrocarbons. *Rsc Advances* 5:62763–62771

[5] Yu M, Zhang N, Fan L, Zhang C, He X, et al. 2015. Removal of organic sulfur compounds from diesel by adsorption on carbon materials. *Reviews in Chemical Engineering* 31:27–43

[6] Lee KX, Valla JA. 2019. Adsorptive desulfurization of liquid hydrocarbons using zeolite-based sorbents: a comprehensive review. *Reaction Chemistry & Engineering* 4:1357–1386

[7] Zhou Y, Li P, Wang Y, Zhao Q, Sun H. 2023. Progress in the separation and purification of carbon hydrocarbon compounds using MOFs and molecular sieves. *Separations* 10:543

[8] Ghadiri M, Ghaemi A, Shayanmehr M. 2026. A comprehensive review on exploring the potential and behavior of carbon-based adsorbents in the adsorptive desulfurization processes. *Fuel* 404:136222

[9] Saha B, Vedachalam S, Dalai AK. 2021. Review on recent advances in adsorptive desulfurization. *Fuel Processing Technology* 214:106685

[10] Dehghan R, Anbia M. 2017. Zeolites for adsorptive desulfurization from fuels: a review. *Fuel Processing Technology* 167:99–116

[11] Yoosuk B, Silajan A, Prasassarakich P. 2020. Deep adsorptive desulfurization over ion-exchanged zeolites: individual and simultaneous effect of aromatic and nitrogen compounds. *Journal of Cleaner Production* 248:119291

[12] Duan J, Pan Y, Liu G, Jin W. 2018. Metal-organic framework adsorbents and membranes for separation applications. *Current Opinion in Chemical Engineering* 20:122–131

[13] Blanco-Brieva G, Campos-Martin JM, Al-Zahrani SM, Fierro JLG. 2011. Effectiveness of metal–organic frameworks for removal of refractory organo-sulfur compound present in liquid fuels. *Fuel* 90:190–197

[14] Cychosz KA, Wong-Foy AG, Matzger AJ. 2008. Liquid phase adsorption by microporous coordination polymers: removal of organosulfur compounds. *Journal of the American Chemical Society* 130:6938–6939

[15] Ullman AM, Brown JW, Foster ME, Léonard F, Leong K, et al. 2016. Transforming MOFs for energy applications using the Guest@MOF concept. *Inorganic Chemistry* 55:7233–7249

[16] Park JH, Ok YS, Kim SH, Cho JS, Heo JS, et al. 2016. Competitive adsorption of heavy metals onto sesame straw biochar in aqueous solutions. *Chemosphere* 142:77–83

[17] Kökçam-Demir Ü, Goldman A, Esrafili L, Gharib M, Morsali A, et al. 2020. Coordinatively unsaturated metal sites (open metal sites) in metal–organic frameworks: design and applications. *Chemical Society Reviews* 49:2751–2798

[18] Van de Voorde B, Hezinová M, Lannoeye J, Vandekerkhove A, Marszalek B, et al. 2015. Adsorptive desulfurization with CPO-27/MOF-74: an experimental and computational investigation. *Physical Chemistry Chemical Physics* 17:10759–10766

[19] Vitillo JG, Regli L, Chavan S, Ricchiardi G, Spoto G, et al. 2008. Role of exposed metal sites in hydrogen storage in MOFs. *Journal of the American Chemical Society* 130:8386–8396

[20] Jia SY, Zhang YF, Liu Y, Qin FX, Ren HT, et al. 2013. Adsorptive removal of dibenzothiophene from model fuels over one-pot synthesized PTA@MIL-101(Cr) hybrid material. *Journal of Hazardous Materials* 262:589–597

[21] Kaur P, Chopra HK. 2022. SBA-15 supported benzoxazolium-based ionic liquids: synthesis, characterization, and application in the adsorptive desulfurization. *Fuel Processing Technology* 238:107480

[22] Luo J, Chao Y, Tang Z, Hua M, Li X, et al. 2019. Design of Lewis acid centers in bundlelike boron nitride for boosting adsorptive desulfurization performance. *Industrial & Engineering Chemistry Research* 58:13303–13312

[23] Xiang Y, Liu Z, Cheng ZL. 2024. Diatomite supported highly-dispersed ZnO/Zn-co-embedded ZIF-8 derived porous carbon composites for adsorption desulfurization. *Journal of Hazardous Materials* 471:134399

[24] Wang C, Lu W, Wu W, Zhang L, Guo W, et al. 2023. Mechanical grinding of FeNC nanomaterial with Fe_3O_4 to construct magnetic adsorbents for desulfurization. *Separation and Purification Technology* 306:122574

[25] He WW, Li SL, Li WL, Li JS, Yang GS, et al. 2013. Multipoint interactions enhanced H_2 storage and organosulfur removal in a microporous metal–organic framework. *Journal of Materials Chemistry A* 1:11111–11116

[26] Huang C, Tong Y, Li J, Peng J, Dong D, et al. 2023. Protonation-induced site and field reconstruction for ultrafast adsorptive desulfurization over Cu–N–C. *Chemical Engineering Journal* 452:139391

[27] Shah SS, Ahmad I, Ahmad W, Ishaq M, Gul K, et al. 2018. Study on adsorptive capability of acid activated charcoal for desulphurization of model and commercial fuel oil samples. *Journal of Environmental Chemical Engineering* 6:4037–4043

[28] Shah SS, Ahmad I, Ahmad W. 2016. Adsorptive desulphurization study of liquid fuels using Tin (Sn) impregnated activated charcoal. *Journal of Hazardous Materials* 304:205–213

[29] Li SL, Lan YQ, Sakurai H, Xu Q. 2012. Unusual regenerable porous metal–organic framework based on a new triple helical molecular necklace for separating organosulfur compounds. *Chemistry* 18:16302–16309

[30] Van de Voorde B, Bueken B, Denayer J, De Vos D. 2014. Adsorptive separation on metal–organic frameworks in the liquid phase. *Chemical Society Reviews* 43:5766–5788

https://doi.org/10.48130/prkm-0026-0017

[31] Maes M, Trekels M, Boulhout M, Schouteden S, Vermoortele F, et al. 2011. Selective removal of N-heterocyclic aromatic contaminants from fuels by Lewis acidic metal–organic frameworks. *Angewandte Chemie (International Edition)* 50:4210–4214

[32] Ghassa M, Khorashe F, Hajjar Z, Soltanali S. 2023. Comparative study on adsorptive desulfurization of thiophenic compounds over terephthalic acid-based and trimesic acid-based metal–organic frameworks. *Energy & Fuels* 37:6490–6502

[33] Gupta NK, Kim S, Bae J, Kim KS. 2021. Chemisorption of hydrogen sulfide over copper-based metal–organic frameworks: methanol and UV-assisted regeneration. *RSC Advances* 11:4890–4900

[34] Kundu M, Hasegawa T, Terabe K, Yamamoto K, Aono M. 2008. Structural studies of copper sulfide films: effect of ambient atmosphere. *Science and Technology of Advanced Materials* 9:035011

[35] Foo KY, Hameed BH. 2010. Insights into the modeling of adsorption isotherm systems. *Chemical Engineering Journal* 156:2–10

[36] Ru J, Wang X, Wang F, Cui X, Du X, et al. 2021. UiO series of metal-organic frameworks composites as advanced sorbents for the removal of heavy metal ions: synthesis, applications and adsorption mechanism. *Ecotoxicology and Environmental Safety* 208:111577

[37] Matoori H, Pour AN, Shadmehri MA. 2025. Adsorptive desulfurization of model fuel by using Co/g-C_3N_4 as an adsorbent. *Progress in Reaction Kinetics and Mechanism* 50:e017

[38] Simonin JP. 2016. On the comparison of pseudo-first order and pseudo-second order rate laws in the modeling of adsorption kinetics. *Chemical Engineering Journal* 300:254–263